RSC Advances

ROYAL SOCIETY OF CHEMISTRY

www.rsc.org/advances

View Article Online
DOI: 10.1039/C5RA11070J

RSC Advances

ARTICLE

Synthesis of new porphyrin/4-quinolone conjugates and evaluation of their efficiency in the photoinactivation of *Staphylococcus aureus*

Received 00th January 20xx,
Accepted 00th January 20xx

DOI: 10.1039/x0xx00000x

www.rsc.org/advances

Pedro N. Batalha[a,b], Ana T. P. C. Gomes[a], Luana S. M. Forezi[b], Liliana Costa[c], Maria Cecília B. V. de Souza[b], Fernanda C. S. Boechat[b*], Vitor F. Ferreira[b], Adelaide Almeida[c], Maria A. F. Faustino[a], Maria G. P. M. S. Neves[a*] and José A. S. Cavaleiro[a*]

Simple methodologies giving access to a new series of pophyrin/4-quinolone conjugates **6** and to the corresponding intra-cyclized derivatives **8** are described. The key steps to obtain **6** involved palladium-catalyzed amination reactions of 6-bromo-4-quinolones containing *N*-ethyl, *N*-pentyl and *N*-ribofuransyl substituents with (2-amino-5,10,15,20-tetraphenylporphyrinato)nickel(II) followed by demetallation. Compounds **8** were obtained from compounds **4**, the nickel(II) complexes of **6**, by an oxidative intracylization approach. The new conjugates were fully characterized and the evaluation of singlet oxygen production showed that these compounds possess good to high capability to generate singlet oxygen. The efficacy of these derivatives to photoinactivate *Staphylococcus aureus*, a Gram-positive bacteria, was evaluated and the best results were obtained with the *N*-ethyl derivatives **8a** and **6a**.

Introduction

Tetrapyrrolic macrocycles like porphyrins play an important role in various fields such as catalysis,[1-3] supramolecular chemistry,[4,5] biomimetic models for photosynthesis,[6-8] electronic materials[9,10] and medicinal chemistry.[11-13]

The medicinal interest on these compounds, namely for photodynamic therapy (PDT) of cancer cells, is related with their ability to act as photosensitizers promoting the formation of reactive oxygen species (ROS), such as singlet oxygen ($^1O_2$), in the presence of light and molecular oxygen. The interaction of these cytotoxic species with cellular components such as lipids, proteins and nucleic acids, in the tissue to be treated is responsible for a cascade of biochemical events that leads to cellular death.[11-13]

PDT involving porphyrins as photosensitizers has been successfully applied to different types of pathologies namely in the diagnosis of neoplastic diseases, treatment of cancer and age related macular degeneration.[13] This approach can be also used to treat infections. The evaluation of porphyrinic photosensitizers effectiveness in the photodynamic inactivation (PDI) of Gram-positive and Gram-negative bacteria, bacterial and fungal endospores, viruses[14-17] and other antimicrobial resistant microorganisms is an important field of research.[18]

Staphylococcus aureus is a bacterium frequently implied in infections, namely superficial infections. For instance, Melo and coworkers[19] found that in clinical samples collected from patients with diabetic foot infections, *S. aureus* was the most common cause of infection and the prevalence and precocity of multidrug resistant (MDR) isolates, namely methicillin-resistant (MRSA), were high. From patients undergoing antibiotic therapy, 93% of the antibiotic regimens were considered to be inadequate based on the antibiotic susceptibility test results. On the other hand, reliable inactivation of *S. aureus* strains has been attained by PDI[20] and the photosensitizing activity is independent of the antibiotic-resistance spectrum of the isolates.

One strategy for obtaining new photosensitizers applicable to PDI consists on the coupling of porphyrins derivatives with pharmacologically active molecules, in a way that target recognition could favour the photosensitizer attachment to the pathogenic microorganism and potentiating a localized photoxidising destructive effect.[21-23]

Knowing the biological activities associated with 4-quinolone derivatives, in particular antibacterial ones,[24-26] herein we report the synthesis of a series of new porphyrin/4-quinolone conjugates **6** and of the corresponding intracyclized derivatives **8** and their efficacy in the photinactivation of *S. aureus,* selected as a model of gram-positive bacteria.

Results and discussion

Synthesis of porphyrin/4-quinolone conjugates

The synthetic strategy to obtain the new porphyrin/4-quinolone conjugates **6** and **8** involved the experimental work

[a] *Department of Chemistry and QOPNA, University of Aveiro, 3810-193 Aveiro, Portugal. E-mail: gneves@ua.pt; jcavaleiro@ua.pt*
[b] *Programa de Pós-Graduação em Química, Instituto de Química, Universidade Federal Fluminense, 24010-141 Niterói, Rio de Janeiro, Brazil. E-mail:nandafarma@gmail.com*
[c] *Department of Biology and CESAM, University of Aveiro 3810-193 Aveiro, Portugal*
† Footnotes relating to the title and/or authors should appear here.
Electronic Supplementary Information (ESI) available: [details of any supplementary information available should be included here]. See DOI: 10.1039/x0xx00000x

View Article Online
DOI: 10.1039/C5RA11070J

summarized in schemes 1-4. The key step was based on the Buchwald-Hartwig reaction between 2-amino-5,10,15,20-tetraphenylporphyrinatonickel(II) (**1**) and the 6-bromo-4-quinolone substrates (**2a-c**).

The amino component was prepared through well established procedures from 5,10,15,20-tetraphenylporphyrin (TPP) through a sequence of Cu(II) complexation, regioselective nitration, demetallation, Ni(II) complexation and nitro-reduction.[27,28]

The 6-bromo-4-quinolone substrates (**2a-c**) (Scheme 1) were obtained from quinolone **3**; this intermediate was prepared from the reaction of *para*-bromoaniline with diethyl ethoxymethylenemalonate, followed by thermic cyclization.[29-32] The subsequent reaction of **3** with bromoethane and 1-bromopentane afforded respectively the ethyl 6-bromo-1-ethyl-4-oxo-1,4-dihydroquinoline-3-carboxylate (**2a**) and ethyl 6-bromo-4-oxo-1-pentyl-1,4-dihydroquinoline-3-carboxylate (**2b**).[33-37] The synthesis of the protected nucleoside derivative, ethyl 1,4-dihydro-1-(2,3,5-tri-*O*-benzoyl-β-D-ribofuranosyl)-4-oxoquinoline-3-carboxylate (**2c**) required the previous treatment of **3** with the silylating agent *N*,*O*-bis(trimethylsilyl)tri-fluoroacetamide (BSTFA) containing 1% of trimethylchlorosilane (TMCS), followed by the reaction with 1-*O*-acetyl-2,3,5-tri-*O*-benzoyl-β-D-ribofuranose in the presence of trimethylsilyltri-fluoromethanesulfonate (TMSOTf) as catalyst.[29]

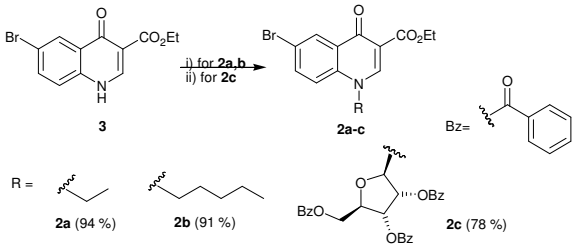

Scheme 1. Synthesis of 6-bromo-4-quinolone substrates **2a-c**. Reaction conditions: i. 1) DMF, K_2CO_3, rt, 15 min. 2) RBr, 80 °C, 24 h.; ii. 1) BSTFA/TMCS, CH_3CN, 70 °C, N_2, 3 h. 2) 1-*O*-acetyl-2,3,5-tri-*O*-benzoyl-β-D-ribofuranose, TMSOTf, rt., 4 h.

In order to select the best ligand, an optimization of the Buchwald-Hartwig reaction conditions was planned using the β-amino porphyrin **1** and the 6-bromo-4-quinolone **2a**. The ligands selected were XPhos, DTPB and *rac*-BINAP (Figure 1) and the experiments were performed in the presence of $Pd(AcO)_2$ and sodium *t*-butoxide (Scheme 2 and Table 1). The selection of this palladium source and of the base was based on previous works.[38,39]

All reactions were carried out in dried toluene, at 110 °C and under nitrogen atmosphere, and the reaction progress was monitored by TLC. The workup involved the washing of the reaction mixture with distillated water, extraction with dichloromethane, fractioning the crude residue with silica gel column and purification with preparative thin layer chromatography. The use of Xphos (Table 1, entry 1) and DTPB (Table 1, entry 2) provided the desired product in acceptable yields (54 and 63% respectively), but after 24 h of reaction the starting porphyrin wasn't completed consumed. The use of *rac*-BINAP (Table 1, entry 3) on the other hand, gave the desired conjugate in excellent yield (89%) with complete consumption of the starting porphyrin, after 6 h. The formation of the byproduct **5** is a result of the transfer of a *rac*-BINAP phenyl group to the metal ion center, followed by a reductive-elimination step during the catalytic cycle.[39]

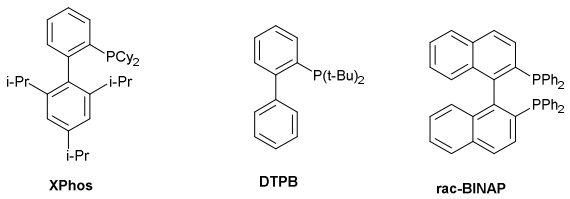

Figure 1. Ligands tested for the palladium catalyzed amination reaction between **1** and **2a**.

Considering the lower reaction time and the excellent yield of the desired conjugate **4a** we considered the presence of that secondary compound **5** as a minor drawback and so the coupling with the other two bromo-quinolones **2b** (Table 1, entry 4) and **2c** (Table 1, entry 5) were performed in the presence of *rac*-BINAP. The reactions provided the desired conjugates **4b** and **4c** in yields of 67% and 63% respectively, with the total consumption of the starting porphyrin. In these cases, unidentified byproducts were also formed and the longer reaction times required for these two bromo-quinolones when compared with those from quinolone **2a** are probably related with steric effects caused by the bulky pentyl and ribofuranosyl groups.

In order to test the applicability of the porphyrin/4-quinolone conjugates as photosensitizers in PDI, it was necessary to perform the demetallation of derivatives **4a-c** (Scheme 3). This procedure was also applied to derivative **5**, which has no quinolone nucleus, but was used for further comparison. With derivative **4c**, the deprotection of the β-ribofuranosyl group was also considered in order to reach a higher hydrophilic character for biological applications.

Conjugates **4a,b** and derivative **5** were demetallated by treatment with sulfuric acid in dichloromethane, affording porphyrins **6a,b** and **7** in excellent yields.

Due to the ribofuranosyl group sensibility to strong acid media, a different approach for obtaining unprotected and demetallated derivative **6c** was applied. Therefore, conjugate **4c** first underwent deprotection of the nucleoside moiety, by treatment with potassium carbonate in a mixture of methanol and ethanol for 48 hours, followed by demetallation with trifluoroacetic acid (TFA), affording the unprotected nucleoside **6c** in 42% yield.

View Article Online
DOI: 10.1039/C5RA11070J

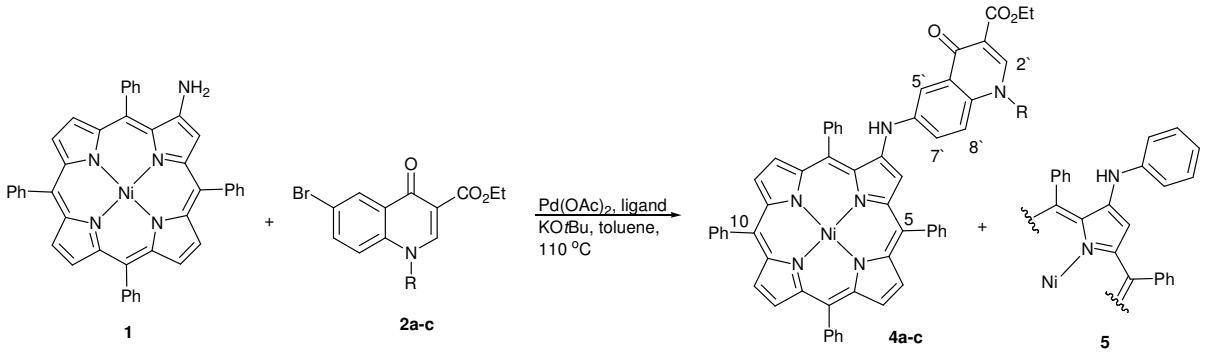

Scheme 2. Buchwald-Hartwig reaction between porphyrin 1 and 6-bromo-4-quinolone derivatives **2a-c**.

Table 1. Ligand and substituent (R) effects on the time and yield of the Buchwald-Hartwig reaction between **1** and **2a-c**.

Entry	R (electrophile)	Ligand	Time (h)	Yield of 4 (%)	Yield of 5 (%)	1 recovered (%)
1	Ethyl (**2a**)	XPhos	24	54	-	7
2	Ethyl (**2a**)	DTPB	24	63	-	9
3	Ethyl (**2a**)	*rac*-BINAP	6	89	8	-
4	Pentyl (**2b**)	*rac*-BINAP	24	67	7	-
5	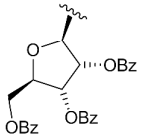 (**2c**)	*rac*-BINAP	72	63	2	-

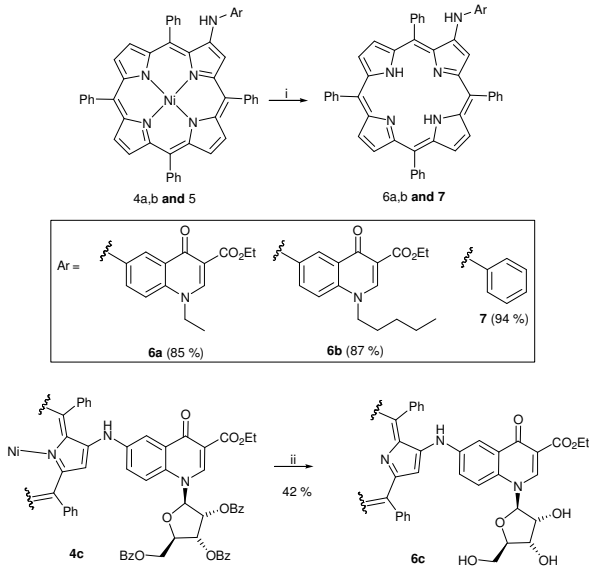

Scheme 3. Demetallation/deprotection of derivatives **4a-c** and **5**. Reaction conditions: i. 1) CH_2Cl_2, H_2SO_4, rt, 10 min. 2) K_2CO_3 (aq) sat.; ii. 1) K_2CO_3, EtOH/MeOH (3:1), rt, 48 h. 2) $CHCl_3$, TFA, rt, 1 h. 3) K_2CO_3 sat.

The possibility of exploring different spectroscopic features from these conjugates **4a,b** *via* an oxidative intracyclization reaction was also outlined (Scheme 4). In fact we have shown that *N*-arylquinolino[2,3,4-*af*]porphyrins obtained through the oxidation of corresponding 2-arylaminoporphyrin show interesting intense absorption bands in the red region of the visible spectrum, and this makes them potential candidates in various scientific areas such as PDT.[38]

The methodology was tested by using both the nickel(II) complex **4a** (Scheme 4, Route A) and the free-base porphyrin **6a** (Scheme 4, Route B). Complex **4a** was fully converted into the corresponding intracyclized derivative after 24 hours in nitrobenzene under reflux, while it took 48 hours to fully convert porphyrin **6a** into the new conjugate **8a.** The higher reactivity associated with complex **4a** is probably due to the planarity of the porphyrinatonickel(II) system, which could energetically favor the cyclization process. The intracyclized intermediate obtained from **4a** after nitrobenzene removal, was demetallated without previous purification, affording derivative **8a** in 60% yield. This procedure was successfully applied to conjugate **4b** and derivative **5**, affording derivatives **8b** and **9** in 56% and 72% yields, respectively. The nucleoside derivative **4c** proved to be rather unstable at the reaction temperature used and therefore its respective intracyclized product could not be obtained. When lower temperatures

View Article Online
DOI: 10.1039/C5RA11070J

were applied to the reaction or even when the oxidizing agent 2,3-dichloro-5,6-dicyanobenzoquinone (DDQ) was added to the mixture, the desired product still could not be obtained.

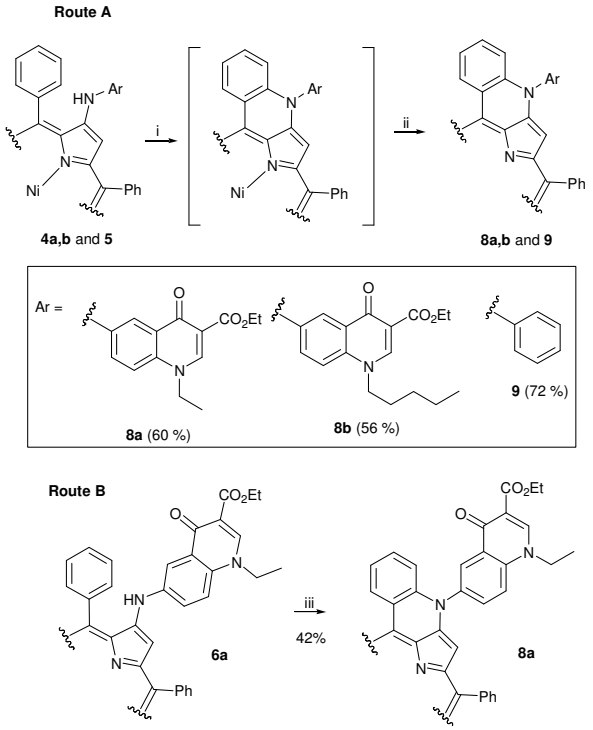

Scheme 2. Oxidative intracyclization reaction from derivatives **4a,b**, **5** and **6a**. Reaction conditions: i. $PhNO_2$, reflux, 24 h.; ii. 1) CH_2Cl_2, H_2SO_4, rt, 10 min. 2) K_2CO_3 sat.; iii. $PhNO_2$, reflux, 48 h.

Structural characterization

The structures of new derivatives **4a-c**, **6a-c** and **8a,b** were assigned according to their UV-Vis, ^1H and ^{13}C NMR spectra and their molecular formulae were confirmed by HRMS. 2D NMR spectra (COSY, HSQC and HMBC) were also used in order to unequivocally identify the proton and carbon resonances.

The absorption spectra of quinolone–porphyrin type derivatives **4a-c** and **6a-c** exhibit intense Soret bands at 411-415 nm and Q-bands at 520-660 nm, being the number of the last ones dependent of the absence or presence of the nickel(II) ion in the porphyrin core while the derivatives **8a,b** show a visible spectra typical of intracyclized macrocycles (see also SI).

The HRMS-ESI$^+$ of the porphyrin/quinolone conjugates **4a** and **4b** show protonated molecular ions $[M+H]^+$ at *m/z* 929.27363 and 971.32075, respectively, confirming the success of the Buchwald-Hartwig. The ^1H NMR spectra of these conjugates show similar patterns considering the resonances of the porphyrin and quinolone protons.

In the ^1H NMR spectrum of conjugate **4a**, for example, it was possible to identify three AB systems at 8.70 and 8.68 ppm, 8.66 and 8.63 ppm and 8.59 and 8.55 ppm with the same coupling constant (*J* = 4.7 Hz) that are related with the resonances of six β-pyrrolic protons. The three singlets at 8.43, 8.35 and 6.48 ppm were assigned to the resonances of H-2', H-3 and N*H*, respectively. The *meso*-phenyl protons appeared as three sets of multiplets at 8.02-7.94 ppm, due to the *ortho* protons of 5,10,15-Ph; at 7.90-7.80 ppm, due to the *ortho* protons of 20-Ph and at 7.74-7.60 ppm, due to the *meta* and *para* protons of 5,10,15,20-Ph. The protons of quinolone core were unequivocally assigned according with the signal multiplicity and the correlations observed in the COSY spectrum. The resonance of quinolone H-5' appeared as a doublet at 7.74 ppm (*J* = 2.6 Hz) as confirmed by the correlation with the double doublet at 7.55 ppm (*J* = 9.0 and 2.6 Hz), assigned to the resonance of H-7'. The correlation observed between the resonance of H-7' and the doublet at 7.32 ppm (*J* = 9.0 Hz) allowed the assignment of this signal to H-8' proton.

A careful analysis of the HMBC spectrum of **4a** allowed the unequivocal assignment of the carbonyl carbon resonances, being the signals at 173.9 and 166.3 ppm assigned to the C-4' and to the carbon from the ester carbonyl group, respectively. Considering the ^1H NMR of conjugate **4b**, the main difference when compared with **4a** spectrum is due to the resonance of the extra aliphatic protons due to the pentyl group attached to *N*-1 (see Supporting Information).

In the case of the porphyrin/ribonucleoside conjugate **4c** the expected *m/z* value at 1345.36388 ($[M+H]^+$) observed in the HRMS-ESI$^+$ spectrum confirmed its molecular formulae. The ^1H NMR spectrum of this compound presents a more complex pattern due to the presence of the protected ribose unit. The multiplets at 8.02-7.95 ppm and at 7.95-7.85 ppm assigned to the resonances of the *ortho* protons of 5,10,15-Ph and 20-Ph, respectively, comprise also the resonances of two *ortho* OBz protons each. The remaining two *ortho* OBz protons appear as a multiplet at 8.77-8.05 ppm. The most prominent difference observed for the quinolone proton resonances was related to H-2' which appeared as a singlet at lower field than in conjugates **4a** and **4b** (8.92 ppm *versus* 8.43 ppm). The COSY spectrum analysis was essential for the unequivocal assignments of the ribose moiety protons (Figure 2). The low field doublet in the aliphatic region at 6.48 ppm (*J* = 4.6 Hz) was attributed to the H-1''. The correlation between this signal with the triplet at 6.01 ppm (*J* = 4.6 Hz) allowed its assignment to H-2''. The H-3'' resonance was identified as the triplet at 5.90 ppm (*J* = 4.6 Hz) due to the correlations observed with H-2'' and with the multiplet at 4.96-4.82 ppm, assigned to the resonances of H-4''and H-5''.

View Article Online
DOI: 10.1039/C5RA11070J

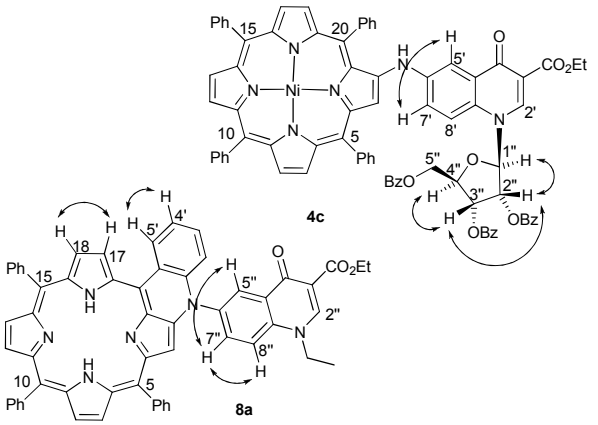

Figure 2. Main COSY correlations of compounds **4c** and **8a.**

An important feature of the ^{1}H NMR spectra of conjugates **6a** and **6b** is the presence of a signal at around -2.60 ppm due to the resonances of the inner N*H* protons, which confirms the success of the demetallation step. In the case of porphyrin/quinolone **6c** it is possible to note also the absence of the signals due to the resonances of the benzoyl groups confirming the presence of deprotected hydroxyl groups. The HRMS-ESI$^+$ of the porphyrin/quinolone conjugates **6a-c** show the expected $[M+H]^+$ molecular ions at the *m/z* values 873.35446, 915.40094 and 977.36557 respectively.

The molecular formulae of the intracyclized *N*-(6-quinolonil)quinolino[2,3,4-*af*]porphyrins **8a** and **8b** were also unambiguously confirmed by HRMS-ESI$^+$ showing the expected $[M+H]^+$ molecular ions at *m/z* values 871.33852 and 913.38539 respectively.

Taking into account the ^{1}H NMR spectrum of derivative **8a**, the presence of two doublets at 9.69 ppm (*J* = 4.7 Hz) and 9.66 ppm (*J* = 8.2 Hz) due to the unshielded protons H-18 and H-5' respectively is consistent with an intracyclized porphyrinic core.[38] Correlations observed on the COSY spectra allowed the identification of the resonance of H-17 as the doublet at 8.83 ppm (*J* = 4.7 Hz) and of H-4' as being in the multiplet at 7.85-7.49 ppm (Figure 2). The electron-withdrawing effect on the protons H-5'' and H-7'', due to the presence of the heteroaromatic ring attached to the C-6'', caused their resonances to appear at a lower field than for derivatives **4a** and **6a**, being related to the doublet at 9.12 ppm (*J* = 2.5 Hz) and to the double doublet at 8.10 ppm (*J* = 8.6 and 2.5 Hz), respectively. The demetallation was also confirmed by the presence of the singlet at -1.32 ppm, related to the two internal N*H* protons. For a more detailed description and NMR spectra see the Supporting Information.

Singlet oxygen generation studies

The efficiency of a photosensitizer either in PDT or PDI is strongly related with its ability to generate reactive oxygen species (ROS), namely singlet oxygen ($^1O_2$) which can initiate oxidative reactions at cellular components level, causing function loss, structure disruption and, consequently, cell death.[16,18-20] Therefore, the potential photodynamic effect of derivatives **6a-c** and **8a,b** was first analyzed by evaluating their ability to generate $^1O_2$. This was accomplished by monitoring the photodecomposition of the yellowish 1,3-diphenylisobenzofuran (DPBF), which reacts with the $^1O_2$ produced through a [4+2] cycloaddition mechanism, affording the colorless 1,2-dibenzoylbenzene.[40-46] The monitoring of the DPBF photodecomposition was made by measuring its absorption decay at 415 nm, on DMF/H_2O (9:1) solutions containing the testing conjugates (0.5 μM) and DPBF (50 μM), while being aerobically irradiated with red light (654 nm ± 20 nm) with an irradiance of 9 mW/cm^2 by using a LED array. *Meso*-tetraphenylporphyrin (TPP), a good singlet oxygen generator, was used as a positive standard in the same conditions.[22] A solution containing DPBF (50 μM), but without photosensitizer was used to evaluate its photodecomposition under the irradiation conditions.

Considering that the structural difference between the synthesized conjugates (**6a-c** and **8a,b**) and the prepared phenyl analogs (**7** and **9**, respectively), relies on the ethyl 4-pyridone-3-carboxylate core present in the quinolone scaffold, derivatives **7** and **9** were also evaluated in order to the further comparison of their photodynamic profile and to understand the role of the quinolone portion in the singlet oxygen generation.

The results of the photodecomposition of DPBF during the irradiation period in the presence of each PS are displayed on Figure 3. The results state that DPBF photodegradation was in general highly enhanced in the presence of the PS conjugates. With the exception of nucleoside derivative **6c**, it was possible to observe that all prepared compounds were capable of generating singlet oxygen. The conjugates **6a,b**, and the phenyl analog **7** display a similar DPBF photodegradation profile although they are slightly less efficient than TPP. A different situation can be observed with the cyclic conjugates **8a,b** and **9** that show a singlet oxygen production higher than that observed for TPP.[47]

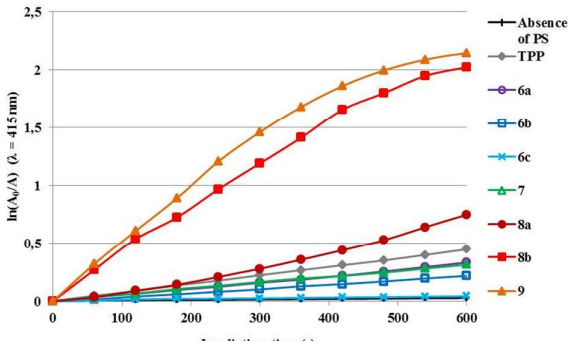

Figure 3. Time dependent photodecomposition of DPBF (50 μM) photosensitized by derivatives **6a-c**, **7**, **8a,b**, **9** and **TPP** in DMF/H_2O (9:1) upon irradiation with red light LEDs (654 nm ± 20 nm) with an irradiance of 9 mW/cm^2 with and without PS (0.5 μM).

View Article Online
DOI: 10.1039/C5RA11070J

Based on these results it was possible to highlight that cyclization has a positive influence on singlet oxygen production of the derivatives probably due to their higher planarity introduced by the intracyclization process.[38,49,50] In addition, it was not found a direct relationship between the alkyl groups attached to the *N*-1 position of the quinolone and the $^1O_2$ production; the low efficiency of nucleoside **6c** to produce singlet oxygen is probably related with molecular aggregation.

Microbial photoinactivation studies

The results obtained from the photoinactivation of Gram-positive bacterium strain *S. aureus* (ATCC 6538) using the quinolones conjugates **6a-c**, **8a,b** and the phenyl analogs **7** and **9** are summarized in Figure 4.

The photoinactivation experiments were performed in phosphate buffered saline (PBS) using a PS concentration of 10.0 μM under white light with an irradiance of 150 W m^{-2}. The results obtained in the dark control (bacterial suspension in the presence of photosensitizer but protected from light exposure) and in the light control (bacterial suspension irradiated with white light in the absence of the photosensitizer) indicate that the reduction on bacterial concentration was due to the photoinactivation treatment. The bacterial concentration in both controls was similar during the experiment (ANOVA, $p > 0.05$).

The concentration of 10.0 μM used in these studies was based on the results obtained from preliminary assays with conjugate **6a** using two different concentrations: 5.0 μM (bacterial inactivation of 2.6 log) and 10.0 μM (bacterial inactivation of 3.1 log) after 120 min under white light irradiation (data not shown). Since the results revealed that the higher concentration (10.0 μM) was the more effective one, all the synthesized compounds were studied at this concentration and the irradiation time was extended to 180 min.

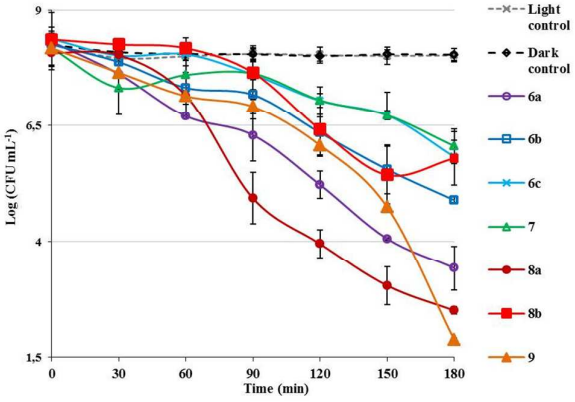

Figure 4. Density variation of *S. aureus* after 30, 60, 90, 120, 150 and 180 min of irradiation, in the presence of 10 μM of different photosensitizers. Each value represents the mean ± standard deviation of three independent experiments, with two replicates each. Error bars represent standard deviations.

The studied photosensitizers revealed clear differences amongst them (ANOVA, $p < 0.05$). The most effective compound was the intracyclized quinolone-conjugate **8a** with rates of inactivation of more than 3 log soon after 90 min of irradiation. At the end of the experiment (180 min) the inactivation rate was of 5.6 log and after 150 min, of 5.0 log (Figure 4). The quinolone-conjugate **6a** was also very effective, showing rates of inactivation of 4.3 and 4.9 log, respectively, after 150 and 180 min. In the presence of **6b** the viability of *S. aureus* decreased 2.7 log after 150 min of irradiation and 3.4 log after 180 min of irradiation. Compounds **6b** and **8b** produced identical rates of inactivation (ANOVA, $p > 0.05$) after 150 min (*ca* 2.6 log) (Figure 4). The non-quinolone intracyclized derivative **9** at the end of the experiment was also effective to inactivate the *S. aureus* with a rate of inactivation of 6.3 log. However, after 150 min of irradiation the inactivation rate was only 3.4 log (Figure 4). The nucleoside derivative **6c** and compound **7** were the least effective showing bacterial reduction of *ca.* 2.1 log after 180 min (Figure 4).

Having into account that according to the American Society of Microbiology, any new approach must achieve a reduction of at least 3 log CFU (killing efficiency of 99.9% or more) to be termed "antimicrobial" or "antibacterial", derivatives **8a**, **6a**, **9**, and even **8b** and **6b**, can be considered effective compounds to be used in PDI of Gram-positive bacteria. However, the rate of inactivation for these five more effective compounds was significantly different after 90 min of treatment, which is due to the PS nature and $^1O_2$ production capability.

The results of this study show that (1) the insertion of quinolone moiety in the porphyrin core, (2) the alteration of the planarity of the macrocycle core by intracyclization and (3) the type of groups and the chain length in the quinolone moiety are key features to be taken into account considering the efficiency of these derivatives in the photoinactivation of *S. aureus*.

The high efficiency of the new intracyclized porphyrin/4-quinolone conjugate **8a** when compared with the others tested PS is probably associated with the ability to produce $^1O_2$ but also with its structural features. Comparing the efficacy of the intracyclized conjugates **8a** (*N*-ethyl substituted quinolone) and **8b** (*N*-pentyl substituted quinolone), the high production of $^1O_2$ observed for compound **8b** is not reflected in a better photoinactivation rate; this suggests that a slight less hydrophobic character of **8a** has also an important role in its efficiency. In fact the ideal PS must possess hydrophilic and hydrophobic character, *i.e.* must be an amphiphilic molecule, in order to improve its photodynamic efficiency.[48] The hydrophobicity is important for the PS to diffuse more easily across the cell membrane and simultaneously it must have some hydrophilic character in order to allow its solubilisation in aqueous medium.

View Article Online
DOI: 10.1039/C5RA11070J

Table 2. Drug-likeness property/Lipinski's 'rule of five' parameters calculated for compounds **6a-c**, **7**, **8a,b** and **9**.[a]

Compound	Molecular Weight	miLog*P*	*n*-ROTB	*n*-O/N	*n*-OH/NH	*n*-violations	Volume	TPSA
6a	873.03	9.88	10	9	3	2	788.98	117.70
6b	915.11	10.09	13	6	3	2	839.39	117.70
6c	977.09	9.61	11	13	6	4	861.93	187.62
7	705.87	9.96	6	5	3	2	645.95	69.39
8a	871.01	9.77	8	9	2	2	778.52	110.61
8b	913.09	10.01	11	9	2	2	828.93	110.61
9	703.85	9.82	4	5	2	2	635.49	62.30

(a) *n*-ROTB, number of rotatable bonds; *n*-O/N, number of hydrogen acceptors; *n*-OH/NH, number of hydrogen bond donors; TPSA, topological polar surface area; *n*-violations, number of violations according to the Lipinski 'rule of five'.

In order to confirm the importance of this feature, the milogP of the compounds was calculated using Molinspiration WebME Editor 3.81 (Table 2).[51] The compounds presented values in the range 9.61–10.01 and as expected the *N*-ethyl substitution conferred a slight less hydrophobic character than the *N*-pentyl substitution.

The less hydrophobic character of PS **8a** when compared with **8b** can enhance its affinity for bacteria,[14,15] and consequently can increase PDI efficiency.[22] The high efficiency of the intracyclized derivative **9** on the production of $^1O_2$ is not also reflected in the rate of inactivation of *S. aureus* in the first 150 min of irradiation. Again, this confirms how important it is the compromise between an efficient $^1O_2$ production and structural features that confer an amphiphilic character to the PS. The results suggest that the $^1O_2$ production capability of **8a** is adequate to inactivate the bacterium *S. aureus*.

Compound **6a** was the second most efficient to inactivate *S. aureus*. This porphyrin/4-quinolone conjugate is not intracyclized and consequently is not so efficient to produce $^1O_2$ as compounds **9**, **8a** and **8b**. However, the presence of the short chain ethyl group attached to the *N*-1' position probably compensates this less $^1O_2$ production drawback and is responsible for a better performance when compared with the pentyl substituted derivatives **8b** and **6b**. The low efficiency of compound **6c** is certainly related with its poor ability to produce $^1O_2$ since it is the less hydrophobic one (miLogP 9.61). Although quinolone conjugate **6a** and phenyl derivative **7** presented similar $^1O_2$ generation capabilities, **6a** is a much more efficient PS, having derivative **7** given a poor rate of inactivation for *S. aureus*. This fact confirms again the importance of the quinolone moiety for the PDI efficiency, considering that due to the $^1O_2$ short lifetime, in the order of microseconds, the PS must be close enough to the bacterial membrane or even inside the cell, to cause efficient cell damage.[48] The similar results obtained in *S. aureus* inactivation by **6b** and **8b** demonstrate that the PS structure planarity also plays an important role in PDI. Even though compound **8b** produces a much higher quantity of $^1O_2$ than compound **6b**, the planarity conferred to the macrocycle by the intracyclization process seems to affect significantly its interaction with the bacterial cell.

Experimental

General

^1H and ^{13}C NMR spectra were recorded on Bruker Avance 300 (300 MHz for ^1H and 75 MHz for ^{13}C), Bruker Avance 500 (500 MHz for ^1H and 125 MHz for ^{13}C) spectrometers. $CDCl_3$ or $CDCl_3/CD_3OD$ were used as solvents and TMS as internal reference and the chemical shifts are expressed in δ (ppm). Unequivocal ^1H assignments were made using 2D COSY, while ^{13}C assignments were made on the basis of 2D HSQC and HMBC experiments (the delay for long-range $J_{C/H}$ couplings were optimized for 7 Hz). HRMS were recorded on a VG AutoSpec M mass spectrometer using $CHCl_3$ as solvent and 3-nitrobenzyl alcohol (NBA) as matrix.

Coupling reactions of porphyrin 1 and bomoquinolones 2a-c. General Procedure.

A mixture of porphyrin **1** (10.0 mg, 14.6 µmol), bromoquinolone **2a-c** (29.2 µmol), KO^tBu (3.5 mg, 31,2 µmol), $Pd(AcO)_2$ (1 mg, 4.5 µmol), *rac*-BINAP (2.3 mg, 3.7 µmol) and dried toluene (5 mL) was purged with N_2 and stirred at 110 °C under N_2 atmosphere until complete consumption of the starting porphyrin (6-48 h, monitored by TLC). After reaching room temperature, the mixture was washed with distilled water and extracted with CH_2Cl_2. The combined organic extracts were evaporated under reduced pressure and the crude mixture was fractioned in a silica gel column, using first CH_2Cl_2 as eluent and then a mixture of CH_2Cl_2/MeOH (20:1). Both fractions were further purified by preparative TLC. The first fraction was purified using a mixture of CH_2Cl_2/petroleum ether (1:1) affording the byproduct **5**. The desired coupling products (**4a-c**) were obtained from the second fraction using

View Article Online
DOI: 10.1039/C5RA11070J

a mixture of CH_2Cl_2/MeOH (20:1). Both products were crystallized from CH_2Cl_2/petroleum ether.

2-(3-Ethoxycarbonyl-1-ethyl-4-oxo-1,4-dihydroquinolin-6-yl-amino)-5,10,15,20-tetraphenylporphyrinatonickel(II) (4a)

Yield: (12.1 mg, 89%). ^{1}H NMR (300 MHz; $CDCl_3$) δ 8.70 and 8.68 (AB, 2H, *J* = 4.7 Hz, H-β), 8.66 and 8.63 (AB, 2H, *J* = 4.7 Hz, H-β), , 8.59 and 8.55 (AB, 2H, *J* = 4.7 Hz, H-β), 8.43 (s, 1H, H-2'), 8.35 (s, 1H, H-3), 8.02-7.94 (m, 6H, H*o*-Ph-5,10,15), 7.90-7.80 (m, 3H, H*o*,*p*-Ph-20), 7.74 (d, 1H, *J*=2,7 Hz, H-5'), 7.74-7.60 (m, 11H, H*m*,*p*-Ph-5,10,15, H*m*-Ph-20), 7.48 (dd, 1H, *J*=9.2 and 2.7 Hz, H-7'), 7.30 (d, 1H, *J* = 9.2 Hz, H-8'), 6.48 (s, 1H, N<u>H</u>), 4.43 (q, 2H, *J* = 7.0 Hz, $CO_2C\underline{H}_2CH_3$), 4.21 (q, 2H, *J* = 7.1 Hz, $NC\underline{H}_2CH_3$), 1.53 (t, 3H, *J* = 7.1 Hz, $NCH_2C\underline{H}_3$) and 1,45 (t, 3H, *J*=7.1 Hz, $CO_2CH_2C\underline{H}_3$) ppm. ^{13}C NMR (75 MHz; $CDCl_3$) δ 173.9 (C-4'), 166.3 ($\underline{C}O_2Et$), 147.2 (C-2'), 145.2, 143.1, 142.9, 142.8, 142.6, 142.1, 141.6, 141.2, 140.9, 140.6, 140.6, 140.2, 139.2, 133.6, 133.6, 133.5, 133.1, 132.9, 132.6, 132.2, 132.1, 131.9, 131.6, 131.5, 130.9, 130.6, 129.4, 128.6, 127.8, 127.7, 127.7, 127.1, 126.9, 120.4, 120.1, 118.6, 116.9, 116.2, 115.8, 113.6, 112.3 (C-3), 109.5, 60.9 ($CO_2\underline{C}H_2CH_3$), 49.0 ($N\underline{C}H_2CH_3$), 14.7 ($NCH_2\underline{C}H_3$), 14.5 ($CO_2CH_2\underline{C}H_3$) ppm. UV-vis (DMF/H_2O (9:1)): λ_{max} (log ε) = 415 (4.94) 537 (4.07) 587 (4.09) nm. HRMS (ESI) *m/z* calcd for $C_{58}H_{43}N_6NiO_3$ $[M+H]^+$ 929.27446, found 929.27363.

2-(3-Ethoxycarbonyl-4-oxo-1-pentyl-1,4-dihydroquinolin-6-yl-amino)-5,10,15,20-tetraphenylporphyrinatonickel(II) (4b)

Yield: (9.5 mg, 67%). ^{1}H NMR (300 MHz; $CDCl_3$) δ 8.70 and 8.69 (AB, 2H, *J* = 4.9 Hz, H-β), , 8.66 and 8.65 (AB, 2H, *J* = 4.9 Hz, H-β), , 8.59 and 8.58 (AB, 2H, *J* = 4.9 Hz, H-β), 8.40 (s, 1H, H-2'), 8.35 (s, 1H, H-3), 8.04-7.96 (m, 6H, H*o*-Ph-5,10,15), 7.93 (d, 2H, *J*=6.9 Hz, H*o*-Ph-20), 7.86 (t, 1H, *J*=7.5 Hz, H*p*-Ph-20), 7.77-7.70 (m, 3H, H*p*-Ph-5,10,15), 7.70-7.61 (m, 9H, H*m* -Ph-5,10,15,20 and H-5'), 7.55 (dd, 1H, *J*=9.0 and 2.7 Hz, H-7'), 7.32 (d, 1H, *J*=9.2 Hz, H-8'), 6.49 (s, 1H, N<u>H</u>), 4.43 (q, 2H, *J* = 7.2 Hz, $CO_2C\underline{H}_2CH_3$), 4.12 (t, 2H, *J*=7.0 Hz, H-1''), 1.95-1.80 (m, 2H, H-2''), 1.45 (t, 3H, *J*= 7.2 Hz, $CO_2CH_2C\underline{H}_3$), 1.42-1.32 (m, 4H, H-3'' and H-4''), and 0.93 (t, 3H, *J*=7.0 Hz, H-5'') ppm. ^{13}C NMR (125 MHz; $CDCl_3$) δ 173.72 (C-4'), 166.42 ($\underline{C}O_2Et$), 147.80 (C-2'), 145.41, 143.16, 142.97, 142.81, 142.71, 142.14, 141.63, 141.27, 141.01, 140.70, 140.65, 140.14, 139.31, 133.68, 133.59, 133.18, 132.91, 132.86, 132.36, 132.13, 131.97, 131.65, 131.57, 130.92, 130.78, 129.40, 128.65, 127.79, 127.73, 127.69, 127.13, 126.94, 120.32, 120.12, 118.61, 116.99, 116.27, 115.85, 113.85, 112.19 (C-3), 109.49, 60.88 ($CO_2\underline{C}H_2CH_3$), 54.17 (C-1''), 28.75 (C-2'' and C-3'' or C-2'' and C-4''), 22.28 (C-3'' or C-4''), 14.55 ($CO_2CH_2\underline{C}H_3$), 13.93 (C-5'') ppm. UV-vis (DMF/H_2O (9:1)): λ_{max} (log ε) = 414 (5.12) 534 (4.05) 588 (4.08) nm. HRMS (ESI) *m/z* calcd for $C_{61}H_{49}N_6NiO_3$ $[M+H]^+$ 971.32141, found 971.32075.

2-[3-Ethoxycarbonyl-1-(2,3,5-tri-O-benzoyl-β-D-ribofuranos-1-yl)-4-oxo-1,4-dihydroquinolin-6-yl-amino)-5,10,15,20-tetraphenylporphyrinatonickel(II) (4c)

Yield: (12.4 mg, 63%). ^{1}H NMR (300 MHz; $CDCl_3$) δ 8.92 (s, 1H, H-2'), 8.70 and 8.69 (AB, 2H, *J* = 4.8 Hz, H-β), 8.67 and 8.66 (AB, 2H, *J*= 4.8 Hz, H-β), 8.66 and 8.59 (AB, 2H, *J* = 4.9 Hz, 8.36 (s, 1H, H-3), 8.11-8.05 (m, 2H, H*o*-OBz), 8.02-7.95 (m, 8H, H*o*-Ph-5,10,15 and H*o*-OBz), 7.95-7.85 (m, 4H, H*o*-OBz and H*o*-Ph-20), 7.85-7.78 (m, 1H, H*p*-Ph-20), 7.77 (d, 1H, *J*=2.5 Hz, H-5'), 7.75-7.61 (m, 11H, H*m*,*p*-Ph-5,10,15 and H*m*-Ph-20), 7.60-7.34 (m, 11H, *Hm,p*-OBz, H-7' and H-8'), 6.48 (d, 1H, *J* = 4.6 Hz, H-1''), 6.41 (s, 1H, N-<u>H</u>), 6.01 (t, 1H, *J*= 4.6 Hz, H-2''), 5.90 (t, 1H, *J*=4.6 Hz, H-3''), 4.96-4.82 (m, 3H, H-4'' and H-5''), 4.31-4.06 (m, 2H, $CO_2C\underline{H}_2CH_3$) and 1.29 (t, 3H, *J*=7.2 Hz, $CO_2CH_2C\underline{H}_3$). ^{13}C NMR (125 MHz; $CDCl_3$) δ 173.82 (C-4'), 166.10 ($\underline{C}OPh$), 165.11 ($\underline{C}OPh$), 164.96 ($\underline{C}O_2Et$), 164.69 ($\underline{C}OPh$), 145.01 (C-2'), 143.14, 142.93, 142.81, 142.47, 142.17, 141.69, 141.34, 140.90, 140.69, 140.64, 139.33, 134.10, 133.90, 133.73, 133.68, 133.60, 132.88, 132.31, 132.26, 132.19, 132.00, 131.67, 131.62, 131.00, 130.13, 129.90, 129.83, 129.77, 129.78, 129.67, 129.31, 129.01, 128.72, 128.67, 128.63, 128.59, 128.55, 128.39, 128.15, 127.93, 127.79, 127.73, 127.15, 127,06, 126.94, 126.92, 120.31, 120.07, 118.64, 116.49, 116.11, 115.89, 113.56, 113.32 (C-3), 110.79 (C-3'), 90.32 (C-1''), 80.83 (C-4'' or C-5''), 74.43 (C-2''), 70.78 (C-3''), 63.46 (C-4'' or C-5''), 60.72 ($CO_2\underline{C}H_2CH_3$), 14.34 ($CO_2CH_2\underline{C}H_3$) ppm. UV-vis (DMF/H_2O (9:1)): λ_{max} (log ε) = 415 (5.21) 538 (4.13) 582 (4.14) nm. HRMS (ESI) *m/z* calcd for $C_{82}H_{59}N_6NiO_{10}$ $[M+H]^+$ 1345.36407, found 1345.36377.

Demetallation of conjugates 4a,b. General Procedure.

To a solution of conjugate **4a,b** (10.8 μmol) in 6 mL of CH_2Cl_2 it was added 600 μL of concentrated H_2SO_4. The mixture was vigorously stirred at room temperature for 10 min and then neutralized with a saturated aqueous solution of K_2CO_3. The resulting mixture was extracted with CH_2Cl_2 and the combined extracts were washed with water and dried over anhydrous Na_2SO_4. The solvent was evaporated under reduced pressure and the desired product was obtained pure after purification by preparative TLC using a mixture of CH_2Cl_2/MeOH (20:1), followed by crystallization with CH_2Cl_2/petroleum ether.

2-(3-Ethoxycarbonyl-1-ethyl-4-oxo-1,4-dihydroquinolin-6-yl-amino)-5,10,15,20-tetraphenylporphyrin (6a)

Yield: (8.0 mg, 85%). ^{1}H NMR (300 MHz; $CDCl_3$) δ 8.84 and 8.79 (AB, 2H, *J* = 4.8 Hz, H-β), 8.78 – 8.73 (m, 3H, H-β), 8.61 (d, 1H, *J*=4.8 Hz, H-β), 8.45 (s, 1H, H-2'), 8.36 (s, 1H, H-3), 8.26-8.15 (m, 8H, H*o*-Ph-5,10,15,20), 8.02-7.95 (m, 1H, H*p*-Ph-20), 7.90-7.82 (m, 2H, H*m*-Ph-20), 7.81 (d, 1H, *J* = 2.7 Hz, H-5'), 7.79-7.72 (m, 9H, H*m*,*p*-Ph-5,10,15), 7.68 (dd, 1H, *J* = 9.2 and 2.7 Hz, H-7'), 7.39 (d, 1H, *J* = 9.2 Hz, H-8'), 6.74 (s, 1H, N<u>H</u>), 4.45 (q, 2H, *J* =7.2 Hz, $CO_2C\underline{H}_2CH_3$), 4.24 (q, 2H, *J* =7.3 Hz, $NC\underline{H}_2CH_3$), 1.56 (t, 3H, *J*=7.3 Hz, $NCH_2C\underline{H}_3$), 1,47 (t, 3H, *J* = 7.2 Hz, $CO_2CH_2C\underline{H}_3$) and -2.60 (bs, 2H, internal N<u>H</u>) ppm. ^{13}C NMR (125 MHz; $CDCl_3$) δ 173.76 (C-4'), 166.38 ($\underline{C}O_2Et$), 147.32 (C-2'), 142.70, 142.19, 141.97, 140.57, 140.30, 140.25, 134.56, 134.41, 134.25, 134.17, 132.98, 132.74, 132.60, 130.74, 129.61, 128.74, 127.75, 127.69, 127.68, 127.47, 127.43, 127.15, 126.89, 126.76, 126.66, 121.48, 120.68 (C-7'), 119.97, 117.92, 116.92, 116.87 (C-8'), 116.60, 114.32 (C-5'), 110.86, 109,82, 60.91 ($CO_2\underline{C}H_2CH_3$), 48.93 ($N\underline{C}H_2CH_3$), 14.75 and 14.56 ppm. UV-vis (DMF/H_2O (9:1)): λ_{max} (log ε) = 411 (5.34) 459 (4.65) 524 (4.27)

View Article Online
DOI: 10.1039/C5RA11070J

571 (3.98) 600 (3.98) 659 (3.52) nm. HRMS (ESI) *m/z* calcd for $C_{58}H_{45}N_6O_3$ $[M+H]^+$ 873.35477, found 873.35446.

2-(3-Ethoxycarbonyl-4-oxo-1-pentyl-1,4-dihydroquinolin-6-yl-amino)-5,10,15,20-tetraphenylporphyrin (6b)

Yield: (8.6 mg, 87%). ^{1}H NMR (300 MHz; $CDCl_3$) δ 8.84 and 8.80 (AB, 2H, *J* = 4.8 Hz, H-β), 8.78 – 8.74 (m, 3H, H-β), 8.62 (d, 1H, *J* = 4.8 Hz, H-β), 8.40 (s, 1H, H-2'), 8.36 (s, 1H, H-3), 8.25-8.16 (m, 8H, H*o*-Ph-5,10,15,20), 8.03-7.95 (m, 1H, H*p*-Ph-20), 7.91-7.83 (m, 2H, H*m*-Ph-20), 7.82 (d, 1H, *J* = 2.7 Hz, H-5'), 7.78-7.70 (m, 9H, H*m*,*p*-Ph-5,10,15), 7.65 (dd, 1H, *J* = 9.2 and 2.7 Hz, H-7'), 7.35 (d, 1H, *J* = 9.2 Hz, H-8'), 6.73 (bs, 1H, N<u>H</u>), 4.45 (q, 2H, *J* = 7.2 Hz, $CO_2C\underline{H}_2CH_3$), 4.12 (t, 2H, *J* = 7.0 Hz, H-1''), 1.95-1.83 (m, 2H, H-2''), 1.46 (t, 3H, *J* = 7.2 Hz, $CO_2CH_2C\underline{H}_3$), 1.43-1.35 (m, 4H, H-3'' and H-4''), 0.94 (t, 3H, *J* = 7.0 Hz, H-5'') and -2.61 (bs, 2H, internal N<u>H</u>) ppm. ^{13}C NMR (125 MHz; $CDCl_3$) δ 173.82 (C-4'), 166.41 ($\underline{C}O_2Et$), 147.85 (C-2'), 142.69, 142.19, 141.97, 141.59, 140.30, 140.25, 138.02, 137.33, 134.56, 134.42, 134.25, 134.17, 132.78, 133.00, 132.60, 130.75, 129.63, 128.75, 127.75, 127.69, 127.66, 127.46, 127.15, 126.89, 126.76, 126.66, 121.48, 120.68, 119.97, 117.92, 116.99, 116.60, 114.29, 110.76, 109.51, 60.92 ($CO_2\underline{C}H_2CH_3$), 54.18 (C-1''), 28.74 (C-2'' and C-3'' or C-2'' and C-4''), 22.28 (C-3'' or C-4''), 14.55 ($CO_2CH_2\underline{C}H_3$) and 13.93 (C-5'') ppm. UV-vis (DMF/H_2O (9:1)): λ_{max} (log ε) = 411 (5.30) 523 (4.21) 571 (3.97) 600 (3.95) 656 (3.56) nm. HRMS (ESI) *m/z* calcd for $C_{61}H_{51}N_6O_3$ $[M+H]^+$ 915.40172, found 915.40094.

Deprotection and demetallation of conjugate 4c.

A solution containing conjugate **4c** (17 mg, 12,6 μmol), K_2CO_3 (3.5 mg, 25.3 μmol), EtOH (1 mL) and MeOH (2 mL) was stirred in the dark under room temperature for 48 h. Then, the solvent was evaporated under reduced pressure and to the obtained residue was added $CHCl_3$ (2 mL) and TFA (300 μL). The mixture was vigorously stirred under room temperature for 1 h, after which it was neutralized with a saturated aqueous solution of K_2CO_3 and extracted with CH_2Cl_2. The combined organic extracts were washed with water and dried over anhydrous Na_2SO_4. The solvent was evaporated under reduced pressure and the product was obtained pure after purification by preparative TLC using a mixture of CH_2Cl_2/MeOH (20:1), followed by crystallization with CH_2Cl_2/petroleum ether.

2-[3-Ethoxycarbonyl-1-(β-D-ribofuranos-1-yl)-4-oxo-1,4-dihydroquinolin-6-yl-amino)-5,10,15,20-tetraphenylporphyrin (6c)

Yield: (5.2 mg, 42%). ^{1}H NMR (300 MHz; $CDCl_3$/CD_3OD) δ 9.13 (s, 1H, H-2'), 8.72-8.65 (m, 3H), 8.63 (d, 1H, *J* = 4.9 Hz, H-β), 8.59 (d, 1H, *J* = 4.9 Hz, H-β), 8.50 (d, 1H, *J* = 4.9 Hz, H-β), 8.36 (s, 1H, H-3), 7.98 (d, 6H, *J* = 6.7 Hz, H*o*-Ph-5,10,15), 7.93-7.86 (m, 1H, H*p*-Ph-20), 7.82-7.52 (m, 15H, H*o,m*-Ph-20, H*m*,*p*-Ph-5,10,15, H-5' and H-8'), 7.40-7.35 (m, 1H, H-7'), 6.49 (s, 1H, N-<u>H</u>), 6.06 (d, 1H, *J*=2.0 Hz, H-1''), 4.39 (q, 2H, *J* = 6.9 Hz, $CO_2C\underline{H}_2CH_3$), 4.33-4.19 (m, 3H, H-2'', H-3'' and H-4''), 4.10 (dd, 1H, *J* = 12.8 and 2.0 Hz, H-5''), 3.94-3.84 (m, 1H, H-5'') and 1.43 (t, 3H, *J* = 6.9 Hz, $CO_2CH_2C\underline{H}_3$). ^{13}C NMR (125 MHz; $CDCl_3$/CD_3OD) δ 174.81 (C-4'), 167.44 ($\underline{C}O_2Et$), 144.71, 143.20, 143.00, 142.89, 142.71, 142.60, 142.26, 141.78, 141.39, 140.91, 140.70, 140.67, 139.37, 133.71, 133.63, 133.61, 133.18, 132.95, 132.54, 132.41, 132.30, 132.23, 132.05, 131.74, 131.70, 130.95, 129.63, 129.19, 128.53, 127.88, 127.81, 127.26, 127.11, 127.09, 126.99, 121.31 (C-7'), 120.18, 118.76, 117.15 (C-5' or C-8'), 116.49, 115.81, 112.90 (C-3), 111.91 (C-8' or C-5'), 108.76, 92.55 (C-1''), 84.68 (C-2''), 75.76 (C-3''), 69.00 (C-4''), 61.44 ($CO_2\underline{C}H_2CH_3$), 60.35 (C-5'') and 14.22 ($CO_2CH_2\underline{C}H_3$) ppm. UV-vis (DMF/H_2O (9:1)): λ_{max} (log ε) = 415 (5.09) 536 (4.02) 583 (4.05) nm. HRMS (ESI) *m/z* calcd for $C_{61}H_{49}N_6O_7$ $[M+H]^+$ 977.36572, found 977.36557.

Oxidative cyclization and demetallation of porphyrin/4-quinolone conjugates 4a,b. General Procedure A.

A solution of conjugate **4a,b** (11.5 μmol) in nitrobenzene (1 mL) was refluxed until complete consumption of the starting material (24 h, monitored by TLC). After reaching room temperature, the solution was solubilized in CH_2Cl_2 and the nitrobenzene removed through elution with CH_2Cl_2 over a short silica gel column. The crude product was recovered by elution with CH_2Cl_2/MeOH (20:1) and solubilized with $CHCl_3$ (6 mL). Concentrated H_2SO_4 (600 μL) was then added to the mixture which was vigorously stirred under room temperature for 10 min. The mixture was neutralized with a saturated aqueous solution of K_2CO_3 followed by extraction with CH_2Cl_2. The combined extracts were washed with water and dried over anhydrous Na_2SO_4. The solvent was evaporated under reduced pressure and the products were purified through preparative TLC using a mixture of CH_2Cl_2/MeOH (20:1), followed by crystallization with CH_2Cl_2/petroleum ether.

***N*-(3-Ethoxycarbonyl-1-ethyl-4-oxo-1,4-dihydroquinolin-6-yl)quinolino[2,3,4-af]-5,10,15-triphenylporphyrin (8a)**

Yield: (6.0 mg, 60%). ^{1}H NMR (300 MHz; $CDCl_3$) δ 9.69 (d, 1H, *J* = 4.7 Hz, H-18), 9.66 (d, 1H, *J* = 8.2 Hz, H-5'), 9.12 (d, 1H, *J* = 2.5 Hz, H-5''), 8.83 (d, 1H, *J* = 4.7 Hz, H-17), 8.75 (d, 1H, *J* = 5.0 Hz, H-β), 8.69 (d, 1H, *J* = 4.4 Hz, H-β), 8.67 (s, 1H, H-2''), 8.65 (d, 1H, *J* = 5.0 Hz, H-β), 8.61 (d, 1H, *J* = 4.5 Hz, H-β), 8.32-8.22, 8.20-8.14 and 8.14-8.04 (3bs, 6H, H*o*-Ph-5,10,15), 8.10 (dd, 1H, *J* = 8.6 and 2.5 Hz, H-7''), 7.85-7.75, 7.75-7.69, 7.69-7.59 and 7.54-7.49 (4m, 14H, H-3, H-2', H-3', H-4', H-8'', H*m*,*p*-Ph-5,10,15), 4.46 (q, 2H, *J* = 7.1 Hz, $CO_2C\underline{H}_2CH_3$), 4.42-4.34 (bs, 2H, $NC\underline{H}_2CH_3$), 1.69 (t, 3H, *J* = 7.2 Hz, $NCH_2C\underline{H}_3$), 1,44 (t, 3H, *J* = 7.1 Hz, $CO_2CH_2C\underline{H}_3$) and -1.32 (bs, 2H, internal N<u>H</u>) ppm. ^{13}C NMR (75 MHz; $CDCl_3$) δ 173.6 (C-4''), 165.8 ($\underline{C}O_2Et$), 149.1 (C-2''), 145.8, 142.4, 142.4, 142.2, 139.0 (C-8a''), 138.2, 138.1, 136.2, 135.3 (C-5'), 134.7, 134.6, 134.5, 134.0, 133.7 (C-7''), 133.6, 132.5, 131.5, 131.4, 129.4 (C-5''), 128.6, 128.54, 127.8, 127.4, 127.2, 126.8, 126.8, 126.7, 126.6, 124.2 (C-18), 123.3, 122.2, 122.1, 122.1, 118.7, 117.3, 116.8, 116.7, 115.2, 111.9, 110.3, 101.3, 61.20 ($CO_2\underline{C}H_2CH_3$), 49.2 ($N\underline{C}H_2CH_3$), 14.7 ($CO_2CH_2\underline{C}H_3$) and 14.4 ($NCH_2\underline{C}H_3$) ppm. UV-vis (DMF/H_2O (9:1)): λ_{max} (log ε) = 412 (5.04) 451 (4.74) 593 (4.15) 610 (4.15) 663 (4.13) nm. HRMS (ESI) *m/z* calcd for $C_{58}H_{43}N_6O_3$ $[M+H]^+$ 871.33912, found 871.33852.

View Article Online
DOI: 10.1039/C5RA11070J

***N*-(3-Ethoxycarbonyl-4-oxo-1-pentyl-1,4-dihydroquinolin-6-yl)quinolino[2,3,4-af]-5,10,15-triphenylporphyrin (8b)**

Yield: (5.9 mg, 56%). ^{1}H NMR (500 MHz; $CDCl_3$) δ 9.70 (d, 1H, *J* = 4.8 Hz, H-18), 9.67 (d, 1H, *J* = 9.8 Hz, H-5'), 9.12 (d, 1H, *J* = 2.4 Hz, H-5''), 8.84 (d, 1H, *J* = 4.8 Hz, H-17), 8.76 (d, 1H, *J* = 4.8 Hz, H-β), 8.70 (d, 1H, *J* = 4.8 Hz, H-β), 8.66 (d, 1H, J = 4.8 Hz, H-β), 8.63-8.60 (ms, 2H, H-β and H-2''), 8.32-8.21, 8.21-8.15 and 8.14-8.06 (2bs and 1m, 7H, H*o*-Ph-5,10,15 and H-7''), 7.85-7.52 (m, 14H, H-3, H-2', H-3', H-4', H-8'', H*m*,*p*-Ph-5,10,15), 4.47 (q, 2H, *J* = 7.0 Hz, $CO_2C\underline{H}_2CH_3$), 4.26 (bs, 2H, H-1''), 2.07-2.00 (m, 2H, H-2''), 1.51-1.43 (m, 7H, H-3'' and H-4'' and $CO_2CH_2C\underline{H}_3$) 1.01 (t, 3H, *J* = 6.7 Hz, H-5'') and -1.31 (bs, 2H, internal N<u>H</u>) ppm. ^{13}C NMR (75 MHz; $CDCl_3$) δ 173.6 (C-4''), 165.8 ($\underline{C}O_2Et$), 149.6 (C-2''), 145.8, 145.4, 142.4, 142.2, 139.1, 138.0, 136.2, 135.2 (C-5'), 134.7, 134.6, 134.5, 134.1, 133.6, 132.5, 131.4, 129.3, 128.6, 128.5, 127.8, 127.4, 127.2, 126.8 (C-17), 126.8, 126.7, 126.6, 124.2 (C-18), 123.3, 122.2, 122.1, 118.8, 117.3, 116.8, 115.2, 111.6, 110.3, 101.4, 61.2 ($CO_2\underline{C}H_2CH_3$), 54.5 (C-1''), 28.8 (C-3'' or C-4''), 28.7 (C-2''), 22.3 (C-3'' or C-4''), 14.5 ($CO_2CH_2\underline{C}H_3$) and 14.0 (C-5'') ppm. UV-vis (DMF/H_2O (9:1)): λ_{max} (log ε) = 412 (5.21) 452 (4.90) 593 (4.31) 610 (4.31) 663 (4.30) nm. HRMS (ESI) *m/z* calcd for $C_{61}H_{49}N_6O_3$ $[M+H]^+$ 913.38607, found 913.38539.

Oxidative cyclization of conjugate 6a. Procedure B.

A solution of conjugate **6a** (10 mg, 11.5 μmol) in nitrobenzene (1 mL) was refluxed until complete consumption of the starting material (48 h, monitored by TLC). After reaching room temperature, it was added CH_2Cl_2 to the reaction mixture and the nitrobenzene was removed through elution with CH_2Cl_2 over a short silica gel column. The crude product was recovered by elution with CH_2Cl_2/MeOH (20:1) and purified through preparative TLC using a mixture of CH_2Cl_2/MeOH (20:1), followed by crystallization with CH_2Cl_2/petroleum ether. Derivative **8a** was isolated in 30% (3.0 mg) yield through this procedure and several unidentified minority byproducts were observed on the TLC analysis.

Singlet oxygen generation

A solution of each PS at a concentration of 0.5 μM in DMF/H_2O (9:1) and 50.0 μM of the singlet oxygen quencher 1,3-diphenylisobenzofuran (DPBF) was irradiated in a glass cuvette, under magnetic stirring at an irradiance of 9.0 mW cm^{-2} with a LED array. The LED array is composed of a matrix of 5 x 5 LED making a total of 25 light sources with an emission peak centred at 654 nm and a bandwidth at half maximum of ± 20 nm. The production of singlet oxygen was evaluated qualitatively through the absorption decay of DPBF at 415 nm for 10 min at defined intervals.[52] The irradiation of the PS in the presence of dissolved oxygen will result in the formation of $^1O_2$, which is trapped by DPBF resulting in colorless *o*-dibenzoylbenzene, after the Diels–Alder like reaction with $^1O_2$.

Bacterial growth conditions

Staphylococcus aureus ATCC 6538 was grown on Brain-Heart Infusion (BHI, Liofilchem, Italy). Before each photodynamic inactivation assay one colony of *S. aureus* was aseptically inoculated into 100 mL of BHI and was grown for 18 h at 37 °C, at 170 rpm stirring. After that, an aliquot of this culture was subcultured in 100 mL of fresh BHI and was grown for 18 h under stirring (170 rpm) at 37 °C to achieve the stationary phase, corresponding to a concentration of approximately 10^8-10^9 colony forming units per mL^{-1} (CFU mL^{-1}).

Photosensitizer stock solutions

For biological assays, 500 μM stock solutions of photosensitizers were prepared in dimethylsulfoxide (DMSO), and diluted to the final concentrations in phosphate buffered saline (PBS, 4 g of NaCl, 0.1 g of KCl, 0.72 g of Na_2HPO_4, 0.12 g of KH_2PO_4 to a final volume of 500 mL and pH 7.4 ± 0.2), depending on the experiment.

Photoinactivation assay

Staphylococcus aureus (ATCC 6538) photoinactivation by the seven porphyrin derivatives, at the concentration of 10.0 μM, was achieved by exposing the *S. aureus* bacterium in laboratory conditions, during defined time intervals, under stirring (100 rpm), to white light at an irradiance of 150 W m^{-2}, provided by an illumination system (LC-122 LumaCare, London) equipped with a halogen 250 W quartz-type lamp and coupled to an interchangeable fiber optic probe (400-800 nm), measured with a Coherent FieldMaxIITop energy meter combined with a Coherent PowerSens PS19Q energy sensor before each photodynamic inactivation assay. Dark and light controls were also included in the experiment. In the light control (LC), the bacterial suspension without photosensitizer was exposed to the same irradiation protocol. In the dark control (DC), the beaker containing the bacterial suspension and the photosensitizer at 10.0 μM was covered with aluminum foil to protect it from any light exposure. Both test and light and dark control beakers were submitted to a pre-irradiation period in the dark during 15 min, at room temperature, to promote the porphyrin/quinolone binding to *S. aureus* cells. Sub-samples of 1.0 mL of test and LC and DC samples were aseptically taken at times 0, 30, 60, 90, 120, 150 and 180 min. The Petri plates were kept in the dark immediately after spreading and also during the incubation. After 48 h of incubation at 37 °C the number of colonies was counted and the rate of bacterial inactivation was evaluated through the quantification of the number of bacteria.[54] Three independent experiments were carried out with two replicates each.

Statistical analysis

Statistical analyses were performed by using SPSS (SPSS 15.0 for Windows, SPSS Inc., USA). Normal distributions were assessed by the Kolmogorov-Smirnov test. The significance of all porphyrins and irradiation time on bacterial inactivation was assessed by two-way univariate analysis of variance (ANOVA) model with the Bonferroni post-hoc test. A value of $p < 0.05$ was considered as significant.

Conclusions

View Article Online
DOI: 10.1039/C5RA11070J

The new pophyrin/4-quinolone conjugates **6** were obtained efficiently via a palladium-catalyzed amination approach that afforded the intracylized conjugates **8** under oxidative conditions. The structures of all conjugates were confirmed by adequate spectroscopic techniques and the ability to generate singlet oxygen was accessed by an indirect method. In general they show good to high ability to generate singlet oxygen, one of the most important requirements for a photosensitizer. The efficacy of these derivatives to photoinactivate the Gram-positive bacterium *S. aureus* was also evaluated and the best bacterial inactivation rates were obtained with the *N*-ethyl derivatives **8a** and **6a.** These compounds showed an important relationship between $^1O_2$ production and their PDI efficiency. Synthesis of similar compounds and the biological assessment considering other types of bacterial pathogens are underway.

Acknowledgements

Thanks are due to the University of Aveiro (Aveiro, Portugal), and Universidade Federal Fluminense (Niterói, RJ, Brazil). We also thank FCT/MEC for the financial support to the QOPNA research Unit (FCT UID/QUI/00062/2013), through national funds and where applicable to those co-financed by the FEDER, within the PT2020 Partnership, to the Portuguese NMR Network and to the FCT-CAPES collaborative programme. Pedro Netto Batalha thanks CAPES for his research grant and for funding his research stay in Aveiro, Portugal (BEX-7131/13-5).

Notes and references

1. C. M. Che and J. S. Huang, *Chem. Commun.*, 2009, 3996.
2. W. Zhang, P. Jiang, Y. Wang, J. Zhang, J. Zheng and P. Zhang, *Chem. Eng. J.*, 2014, **257**, 28.
3. G. Silva, S. M. G. Pires, V. L. M. Silva, M. M. Q. Simões, M. G. P. M. S. Neves, S. L. H. Rebelo, A. M. S. Silva and J. A. S. Cavaleiro, *Catal. Commun.*, 2014, **56**, 68.
4. C. J. Medforth, Z. Wang, K. E. Martin, Y. Song, J. L. Jacobsen and J. A. Shelnutt, *Chem. Commun.*, 2009, 7261.
5. R. Gautam and S. M. S. Chauhan, *Mat. Sci. Eng. C*, 2014, **43**, 447.
6. H. Imahori, Y. Mori and Y. Matano, *J. Photoc. Photobio. C*, 2003, **4**, 51.
7. G. Bottari, O. Trukhina, M. Ince and T. Torres, *Coordin. Chem. Rev.*, 2012, **256**, 2453.
8. L. L. Li and E. W. G. Diau, *Chem. Soc. Rev.*, 2013, **42**, 291.
9. M. Jurow, A. E. Schuckman, J. D. Batteas and C. M. Drain, *Coordin. Chem. Rev.*, 2010, **254**, 2297.
10. A. Han, H. Jia, H. Ma, S. Ye, H. Wu, H. Lei, Y. Han, R. Cao and P. Du, *Phys. Chem. Chem. Phys.*, 2014, **16**, 11209.
11. A. P. Castano, T. N. Demidova and M. R. Hamblin, *Photodiagn. Photodyn.*, 2004, **1**, 279.
12. E. S. Nyman and P. H. Hynninen, *J. Photoc. Photobio. B*, 2004, **73**, 1.
13. K. M. Kadish, K. M. Smith and R. Guillard, in *The Porphyrin Handbook*, Academic Press, San Diego, 2000.
14. M. R. Hamblon and T. Hasan, *Photoc. Photobio. Sci.*, 2004, **3**, 436.
15. X. Fu, Y. Fang and M. Yao, *Biomed Res. Int.*, 2013, 1.
16. M. Q. Mesquita, J. C. J. M. D. S. Menezes, M. G. P. M. S. Neves, A. C. Tomé, J. A. S. Cavaleiro, Â. Cunha, A. Almeida, S. Hackbarth, B. Röder and M. A. F. Faustino, *Bioorg. Med. Chem. Lett.*, 2014, **24**, 808.
17. L. Costa, J. P. C. Tomé, M. G. P. M. S. Neves, A. C. Tomé, J. A. S. Cavaleiro, M. A. F. Faustino, Â. Cunha, N. C. M. Gomes and A. Almeida, *Antivir. Res.*, 2011, **91**, 278.
18. J. Almeida, J. P. C. Tomé, M. G. P. M. S. Neves, A. C. Tomé, J. A. S. Cavaleiro, Â. Cunha, L. Costa, M. A. F. Faustino and A. Almeida, *Photoc. Photobio. Sci.*, 2014, **13**, 626.
19. J. J. Mendes, A. Marques-Costa, C. Vilela, J. Neves, N. Candeias, P. Cavaco-Silva and J. Melo-Cristino, *Diabetes Res. Clin. Pr.*, 2012, **95**, 153.
20. A. Almeida, Â. Cunha, M. A. F. Faustino, A. C. Tomé and M. G. P. M. S. Neves, In *Photodynamic Inactivation of Microbial Pathogens: Medical and Environmental Applications.*, ed. Hamblin MR, Jori G, Royal Society of Chemistry, Cambrige, 2011, pp. 83-160.
21. F. C. Santos, A. C. Cunha, M. C. B. V. de Souza, A. C. Tomé, M. G. P. M. S. Neves, V. F. Ferreira and J. A. S. Cavaleiro, *Tetrahedron Lett.*, 2008, **49**, 7268.
22. A. T. P. C. Gomes, A. C. Cunha, M. R. M. Domingues, M. G. P. M. S. Neves, A. C. Tomé, A. M. S. Silva, F. C. Santos, M. C. B. V. de Souza, V. F. Ferreira and J. A. S. Cavaleiro, *Tetrahedron*, 2011, **67**, 7336.
23. M. M. Bastos, A. T. P. C. Gomes, M. G. P. M. S. Neves, A. M. S. Silva, O. A. Santos-Filho, N. Boechat and J. A. S. Cavaleiro, *Eur. J. Org. Chem.*, 2013, 1485.
24. A. Ahmed and M. Daneshtalab, *J. Pharm. Pharm. Sci.*, 2012, **15**, 52.
25. L. Mitscher, *Chem. Rev.*, 2005, **105**, 559.
26. C. Mugnaini, S. Pasquini and F. Corelli, *Curr. Med. Chem.*, 2009, **16**, 1746.
27. H. K. Hombrecher, V. M. Gherdan, S. Ohm; J. A. S. Cavaleiro, M. G. P. M. S. Neves and M. F. Condesso, *Tetrahedron*, 1993, **49**, 8569.
28. S. Richeter, C. Jeandon, J. P. Gisselbrecht, R. Graff, R. Ruppert and H. J. Callot, *Inorg. Chem.*, 2004, **43**, 251.
29. C. V. B. S. Canuto, C. R. B. Gomes, I. P. Marques, L. V. Faro, F. C. Santos, I. C. P. P. Frugulhetti, T. M. L. Souza, A. C. Cunha, G. A. Romeiro, V. F. Ferreira and M. C. B. V. de Souza, *Lett. Drug Des. Discov.*, 2007, **4**, 404.
30. W. M. Lauer, R. T. Arnold, H. Tiffany and J. Tinker, *J. Am. Chem. Soc.*, 1946, **68**, 1268.
31. V. G. Ramsey and L. H. Cretcher, *J. Am. Chem. Soc.*, 1947, **69**, 1659.
32. B. Riegel, G. R. Lappin, B. H. Adelson, R. I. Jackson, C. J. Albisetti, R. M. Dodson and R. H. Baker, *J. Am. Chem. Soc.*, 1946, **68**, 1264.
33. C. Mugnaini, S. Nocerino, V. Pedani, S. Pasquini, A. Tafi, M. de Chiaro, L. Bellucci, M. Valoti, F. Guida, L. Luongo, S. Dragoni, A. Ligresti, A. Rosenberg, D. Bolognini, M. G. Cascio, R. G. Pertwee, R. Moaddel, S. Maione, V. S. di Marzo and F. Corelli, *Chemmedchem*, 2012, **7**, 920-934.
34. S. Pasquini, A. Ligresti, C. Mugnaini, T. Semeraro, L. Cicione, M. de Rosa, F. Guida, L. Luongo, M. de Chiaro, M. G. Cascio, D. Bolognini, P. Marini, R. Pertwee, S. Maione, V. di Marzo and F. Corelli, *J. Med. Chem.*, 2010, **53**, 5915.
35. S. Pasquini, C. Mugnaini, C. Tintori, M. Botta, A. Trejos, R. K. Arvela, M. Larhed, M. Witvrouw, M. Michiels, F. Christ, Z. Debyser and F. Corelli, *J. Med. Chem.*, 2008, **51**, 5125.
36. S. Pasquini, M. de Rosa, A. Ligresti, C. Mugnaini, A. Brizzi, N. P. Caradonna, M. G. Cascio, D. Bolognini, R. G. Pertwee, V. di Marzo and F. Corelli, *Eur. J. Med. Chem.*, 2012, **58**, 30.
37. S. Pasquini, M. de Rosa, V. Pedani, C. Mugnaini, F. Guida, L. Luongo, M. de Chiaro, S. Maione, S. Dragoni, M. Frosini, A. Ligresti, V. di Marzo and F. Corelli, *J. Med. Chem.*, 2011, **54**, 5444.
38. A. M. V. M. Pereira, C. M. A. Alonso, M. G. P. M. Neves, A. C. Tomé, A. M. S. Silva, F. A. A. Paz and J. A. S. Cavaleiro, *J. Org. Chem.*, 2008, **73**, 7353.

View Article Online
DOI: 10.1039/C5RA11070J

39. J. C. J. M. D. S. Menezes, A. M. V. M. Pereira, M. G.P. M. S. Neves, A. M. S. Silva, S. M. Santos, S. T. Martínez, B. V. Silva, A. C. Pinto and J. A. S. Cavaleiro, *Tetrahedron*, 2012, **68**, 8330.
40. I. Walker, S. A. Gorman, R. D. Cox, D. I. Vernon, J. Griffiths and S. B. A. Brown, *Photoc. Photobio. Sci.*, 2004, **3**, 653.
41. L. Roitman, B. Ehrenberg and N. Kobayashi, *J. Photoc. Photobio. A*, 1994, **77**, 23.
42. C. Hadjur, N. Lange, J. Rebstein, P. Monnier, H. van den Bergh and G. Wagnieres, *J. Photoc. Photobiol. B*, 1998, **45**, 170.
43. M. Krieg, *J. Biochem. Bioph. Meth.*,1993, **27**, 143.
44. P. Zimcik, M. Miletin, H. Radilova, V. Novakova, K. Kopecky, J. Svec and E. Rudolf, *Photochem. Photobiol.*, 2010, **86**, 168.
45. L. M. Rossi, P. R. Silva, L. L. R. Vono, A. U. Fernandes, D. B. Tada and M. S. Baptista, *Langmuir*, 2008, **24**, 12534.
46. M. B. Spesia, A. E. Milanesio and E. N. Durantini, *Eur. J. Med. Chem.*, 2008, **43**, 853.
47. A. A. Krasnovsky, *P. Roy. Soc. Edinb. B.,* 1994, **102**, 219.
48. F. M. Engelmann, S. V. O. Rocha, H. E. Toma, K. Araki and M. S. Baptista, *Int. J. Pharm.*, 2007, **329**, 12.
49. S. Richeter, C. Jeandon, J.-P. Gisselbrecht, R. Graff, R. Ruppert and H. J. Callot, *Inorg. Chem.*, 2004, **43**, 251.
50. D.-M. Shen, C. Liu and Q.-Y. Chen, *Eur. J. Org. Chem.*, 2007, 1419.
51. The parameters for drug-likeness were evaluated according to the Lipinski's 'rule-of-five', using the MolinspirationWebME Editor 3.81., http://www.molinspiration.com (accessed May 2015).
52. W. Spiller, H. Kliesch, D. Wöhrle, S. Hackbarth, B. Röderand and G. Schnurpfeil, *J. Porphyr. Phtalocya.*, 1998, **2**, 145.
53. E. Alves, L. Costa, C. M. B. Carvalho, J. P. C. Tomé, M. A. Faustino, M. G. P. M. S. Neves, A. C. Tomé, J. A. S. Cavaleiro, Â. Cunha and A. Almeida, *BMC Microbiol.*, 2009, **9**, 70.

View Article Online
DOI: 10.1039/C5RA11070J

Synthesis of new porphyrin/4-quinolone conjugates and evaluation of their efficiency in the photoinactivation of *Staphylococcus aureus*

Pedro N. Batalha[a,b], Ana T. P. C. Gomes[a], Luana S. M. Forezi[b], Liliana Costa[c], Maria Cecília B. V. de Souza[b], Fernanda C. S. Boechat[b*], Vitor F. Ferreira[b], Adelaide Almeida[c], Maria A. F. Faustino[a], Maria G. P. M. S. Neves[a*], José A. S. Cavaleiro[a*]

[a] *Department of Chemistry and QOPNA, University of Aveiro, 3810-193 Aveiro, Portugal*

[b] *Programa de Pós-Graduação em Química, Instituto de Química, Universidade Federal Fluminense, 24010-141 Niterói, Rio de Janeiro, Brazil.*

[c] *Department of Biology and CESAM, University of Aveiro 3810-193 Aveiro, Portugal*

Table of Contents

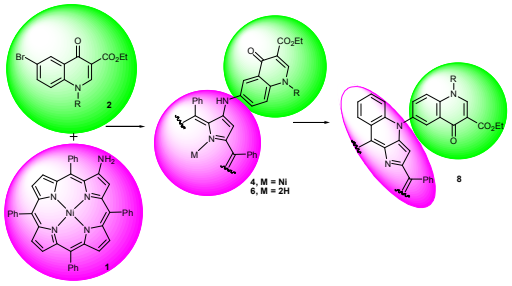

The synthesis of new porphyrin/4-quinolone conjugates and their evaluation as potential photosensitizers in the photoinactivation of *Staphylococcus aureus* is described.